Brookhaven National Laboratory

Associated Universities Incorporated

Upton, New York 11973

Muon g–2 Note No. 29

Title: The Inflection Path into the g-2 Storage Ring

Author: H. N. Brown

Affiliation: Brookhaven National Laboratory

Date: June 28, 1989

[illegible]

28 June 1989
H. N. Brown

THE INFLECTION PATH INTO THE G-2 STORAGE RING

This note examines the deflections of the injected beam as it passes through the varying magnetic fields of the ring and inflector, with a view toward determining acceptable ring and beam hole orientations for either clockwise or counter-clockwise injection. Recommendations are made for the coordinates of the ring center and for a standard reference bearing in the G-2 building. Based on these, definitive beam approach bearings and coordinates are then given for each case. In addition, the focussing effect of the fringing field is examined, the beam rematched via the last 4 quadrupoles, and the required pipe sizes leading to the inflector evaluated. Horizontal steering capabilities are briefly noted.

I. INJECTION TRAJECTORY

The incoming pion (or muon) beam must pass somehow through the fringing field of the storage ring. It is the function of the inflector to make this possible. In order to design and position the inflector, the fringing field effects must be examined in detail. To do this, a Fortran program named INFLECT.FOR was written. It requires input data describing the fringe field of the storage ring. The program POISSON has been employed in the ring design to calculate the vertical field By as a function of radius r. For a given tangential reference axis, the radial map can be used to find the field as a function of distance along the axis. John Jackson has supplied a POISSON output file using the most recent magnet parameters. This data was scaled up by a factor 1.0109 to exactly match the the "magic" momentum 3.0944 GeV/c and the storage orbit radius R0= 280 inches = 7.112 meters. Figure I.1 is a plot of the vertical field By vs the distance s along a reference axis which is tangent to the ring at a radius (R0 + 75 mm).

Because of the small aperture of the inflector, in comparison to the characteristic dimension of the storage ring's magnetic field, it is not possible to make the field near zero everywhere along the injection trajectory. The field due to the inflector falls off to zero within 5 cm or so from the ends, while the main fringing field requires 20 times that distance to reach zero. Figure I.1 shows that there will be pronounced curvature of the trajectory before and after entering an inflector whose length is approximately equal to the effective length of the fringing field. An optimum path and/or inflector orientation can be selected to minimize the amount of inflector aperture used up by this curvature in a straight device, or else the inflector can be bent to follow the curve, preserving all the aperture.

Several examples of input trajectories have been calculated by INFLECT with respect to the reference axis defined above. They are shown in the following figures. (INFLECT.FOR was verified to be working correctly by checking it against an artificial field map through which the trajectory could be analytically integrated.)

Input Angle	Inflector Length 1.6 m	1.7m	1.8 m
Ø. Deg	Fig I.2a	Fig I.3a	Fig I.4a
1.25 Deg	Fig I.5a	Fig I.6a,b,c,d	Fig I.7a

Fig. a in each case shows the trajectory in detail as it approaches and passes through the inflector. The input angle is positive outward with respect to the tangential reference axis. The solid curve is the trajectory of a central beam particle. The solid straight lines depict the assumed apertures (18 mm H x 45 mm V for the inflector). The dashed lines are the aperture center lines. The dotted curve is the departure of the trajectory from the aperture centerline. These figures show that, with respect to the amount of aperture used by the curving path in the (assumed) straight inflector, it is advantageous to use a longer inflector length and to enter the back leg at an outgoing angle. Obviously, the longer inflector requires a lower field. In addition, the outgoing approach angle also reduces the required inflector field. Figure I.6c illustrates the effect of curving the inflector to a radius of 125 meters. The departure from the axis is reduced to less than +-Ø.4 mm, in comparison to +-1.9 mm for the straight case of Figure I.6a.

Figure I.6b shows, on a larger scale, how the arrangement fits through the back leg steel with respect to the two adjacent bolt holes. It is assumed that the radius through s=Ø passes 1.25 degrees ccw from a bolt hole center, allowing a generous clearance for current feed at the exit of the inflector (see Figure II.1). The outer "circle" represents the outer edge of the back leg; the middle "circle" represents the inner edge of the back leg where the main fringe field begins; the inner "circle" represents the outer edge of the pole piece.

Figure I.6d illustrates typical vertical motion of a particle crossing the median plane at the entrance to the back leg at an angle of 1Ø mrad.

II. RING LOCATION AND ORIENTATION

Frank Karl has established the location of various points in the G-2 Storage Ring building in the AGS grid system. He has selected a point midway between the NW and SE wall columns, and 4ØØ" from the SW wall columns which closely matches the ring center assumed in the magnet design work up to now. That center point is:

$$\begin{pmatrix} 1953Ø.627\text{" North} \\ 5Ø55.694\text{" East} \end{pmatrix}$$

Furthermore, he has determined the bearing of the centerline of the building (along the "spine") to be North 29.8989° East. Frank Karl and Irv Polk have agreed to adopt, for simplicity, the bearing

North 30.000° East

as the defining direction for orienting the ring. The difference with respect to the measured angle, 0.1011° represents a run-out of only 1.1" across the ring diameter.

Data on the design of the storage ring's steel core has been supplied by Mike Papianos. The ring's 30° sectors can be arranged symmetrically with the N 30 E line through the center of a sector, as has been done up to now. It is desirable to bring the beam into the ring without changing the total bend (46°) in D5 and D6 by very much. Figure II.1 depicts acceptable reference axes (still displaced 75mm outside R0) which satisfy this requirement for clockwise and for counter-clockwise injection. All the cases illustrated in Figures I.2 to I.7 apply to these axes and in each case the beam hole perimeter lies at least 40mm from the closest bolt hole perimeter.

Since the increased duty factor for the inflector (3 pulses per AGS cycle compared to 1 for the CERN experiment) and the longer fringing field already stress the inflector design considerably, we should endeavor to minimize the inflector field as much as possible. The effective length of the fringe field is about 1.92 meters. An inflector of this length would protrude too far into the cryostat of the main coils. Frank Krienen's scale model of the magnet and cryostat demonstrates that a length of even 1.8 meters would require a "dimple" in the cryostat wall. Consequently, it is recommended, on the basis of this work, that an inflector effective length of 1.7 meters and an outward beam angle of 1.25° with respect to the reference axes shown in Figure II.1 be used.

Figures I.2-I.7 pertain to $x=0$, $x'=0$ at the injection point $s=0$. Capture efficiency studies by Walter Lysenko indicate that an injection angle of $x'=0$ is best for muon injection but that for pion injection there is a broad optimum at $x'=-3.5$ mrad. In order to define a beam axis now, let us use $x=0$, $x'=-1.75$ mrad as the constraint at $s=0$. (This shifts the beam axis in the figures of Section I by only a milli-meter or two.) Clockwise injection was assumed in Figs. I.2-I.7, but a mirror inversion makes them applicable to ccw injection as well. Figure II.2 shows, for both directions of rotation, beam axes for this last constraint based on the 1.7 m inflector and 1.25° approach of Figures I.6a,b,c,d. Bearings and coordinates are indicated in the tangential reference axis system and in the AGS grid system and may be used to locate the beam hole axis in the back leg of the magnet. The exact positiong of the inflector must await decisions on its final form.

III. INJECTION FOCUSSING EFFECTS

Since there is a substantial gradient in the fall-off region of the main ring field, off-axis particles experience important horizontally defocussing and vertically focussing forces. In what follows, the horizontal motion is calculated only in the median plane, using the actual field at each point. The vertical motion is calculated from the first order field at each point Bx=G*y=(dBx/dy)*y, where x and y are normal to the reference axis s, and dBx/dy is obtained from the tabulated values of dBy/dr (=dBr/dy) in the POISSON file, taking account of the angle between the r and x directions at each point. Figure III.1 shows G on the axis as a function of s. The integral of this gradient is 5.71 Tesla, which at 3.1 Gev/c makes the fringing field approximately equivalent to a lens of 1.8 meter focal length.

An effective transform matrix is derived by following several representative rays. These transform matrices were derived for the case shown in Figures I.6a,b,c,d (i.e., 1.7 m inflector length, 1.25° approach angle). It is convenient to represent them as a drift-matrix-drift, where the total drift is equal to the distance from s=-3.898 m (the entrance to the backleg) to s=0. The first drift is chosen to place the matrix near the center of the focussing region at s=-1.8 m. We then have:

(H12,V12 in meters, H21,V21 in 1/m)

$$H = \begin{pmatrix} 1. & 1.8 \\ 0. & 1. \end{pmatrix} \begin{pmatrix} .99400 & -.11291 \\ .61700 & .93603 \end{pmatrix} \begin{pmatrix} 1. & 2.098 \\ 0. & 1. \end{pmatrix}$$

$$V = \begin{pmatrix} 1. & 1.8 \\ 0. & 1. \end{pmatrix} \begin{pmatrix} .93692 & .14854 \\ -.48990 & .98981 \end{pmatrix} \begin{pmatrix} 1. & 2.098 \\ 0. & 1. \end{pmatrix}$$

As one might expect, H and V are equivalent to fairly thin (~0.1m) defocussing and focussing lenses at the chosen location. These transformations were then employed in the program TRANSPORT to rematch the beam emittance parameters to the values desired at the entrance to the storage ring. Figure III.2a illustrates the matched beam envelopes which were formerly obtained without taking account of the main fringe field. (We apologize for the change in units.) Figure III.2b shows the rematched envelopes. There is a small discontinuity in the envelopes near the inflector entrance due to the point transformations above which were inserted there. Because of the strong vertical focussing, it is now necessary to bring the beam to a small vertical waist near the entrance to the back leg so that it can then expand and be left in an approximate parallel condition by the fringe gradient (See Fig. I.6d). The horizontal change is reflected in the need to now bring the beam to a greater width at the last quad (Q29) to make it converge strongly toward a small waist which is then shifted by the defocussing gradient down to the inflector exit as desired.

The nominal beam sizes in the inflector do not change. However, the nominal horizontal beam diameter at the entrance to the back leg increases from 2.2" to 3.2". Consequently, we must plan on a 4" pipe through the back leg steel. The pipe size from the inner edge of the back leg to the inflector is fixed by the horizontal beam size also, which is now a nominal 2.0". The pipe there should be at least 3".

Since the integrated fields of the inflector and ring very nearly cancel, the net momentum dispersion due to them is small. At the inflector exit, for the case of Figure I.6, it is

$$\begin{pmatrix} dx \\ dx' \end{pmatrix} = \begin{pmatrix} 58 \text{ mm} \\ 27 \text{ mrad} \end{pmatrix} dp/p$$

which is negligible for the dp/p ~ +-.006 of interest here.

IV. BEAM STEERING

This paragraph will just touch on horizontal beam steering adjustments. (Vertical steering depends on dipoles which are upstream of one or more quads and will not be analyzed here.) Assuming that the beam has been satisfactorily brought to the center of the last quad (Q29) by upstream manipulations, the final steering into the ring can be accomplished by adjusting the deflections in the last horizontal steering dipole (between Q29 and the ring) and in the inflector. The H matrix of Section III may be employed to find the changes in x and x' at the inflector exit. Letting As and Ai be the deflections in the steerer and the inflector, inverting the calculation gives:

$$\begin{pmatrix} dAs \\ dAi \end{pmatrix} = \begin{pmatrix} .1895 \text{ mrad/mm} & -.1611 \\ -.5104 \text{ mrad/mm} & 1.4338 \end{pmatrix} \begin{pmatrix} dx \\ dx' \end{pmatrix}$$

Thus, the beam can be moved by 5 mm or 5 mrad by means of about 1 mrad changes in the steerer and 7 mrad in the inflector. The steering magnet requirement is typical of that for all the other vernier dipoles in the line. The inflector can easily make such a change since its field is equivalent to some 240 mrad of bend. Such displacements would, of course, use up 4-5 mm of inflector aperture. Thus, it will be easy to optimize the capture as a function of x, x' within the transmission limits of the inflector.

Fig. I.1 variation of Main Fringe Field along the Tangential Reference Axis.

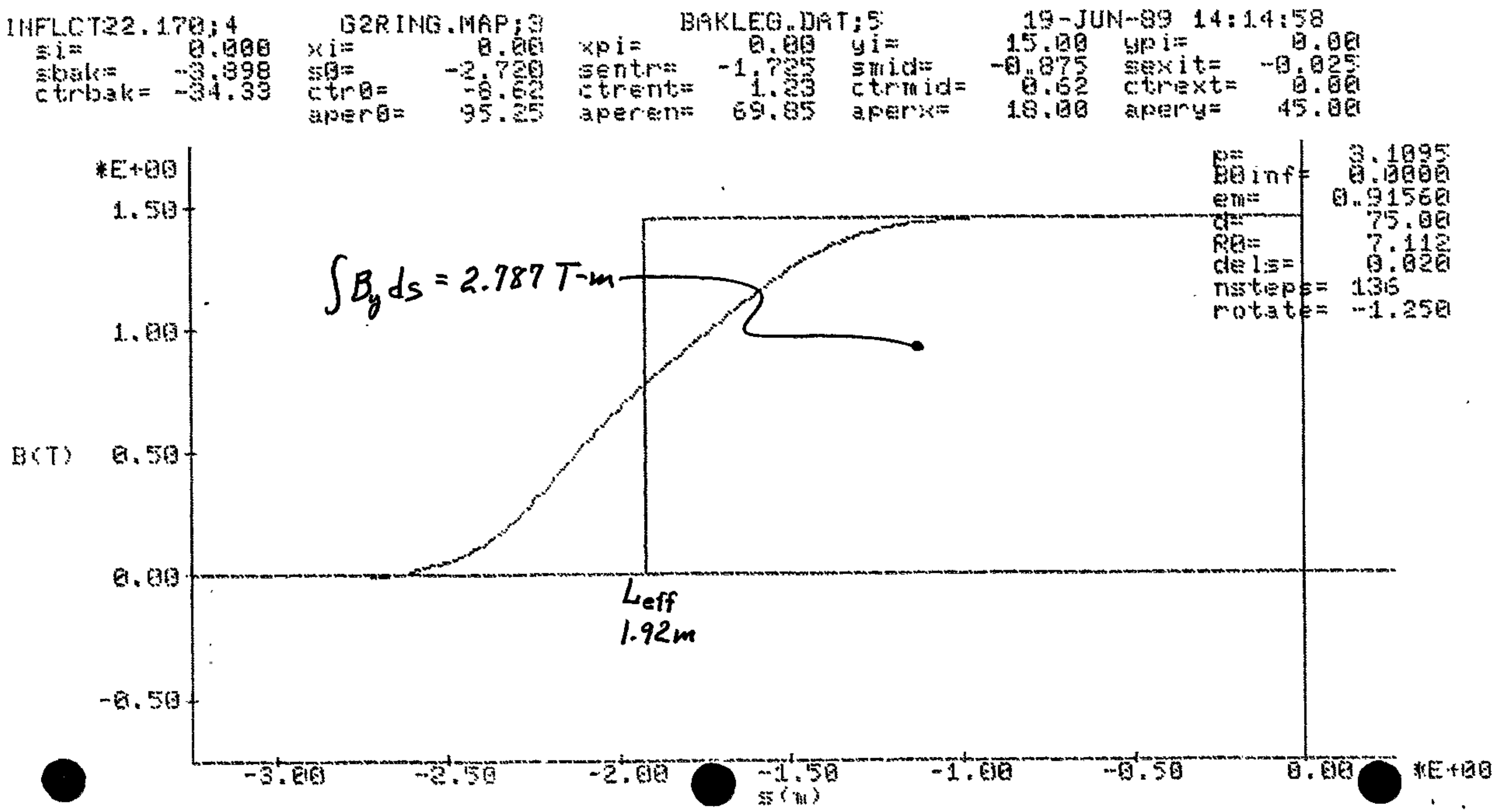

Fig. I.2a Trajectory for 1.6 m Inflector, 0° Approach.

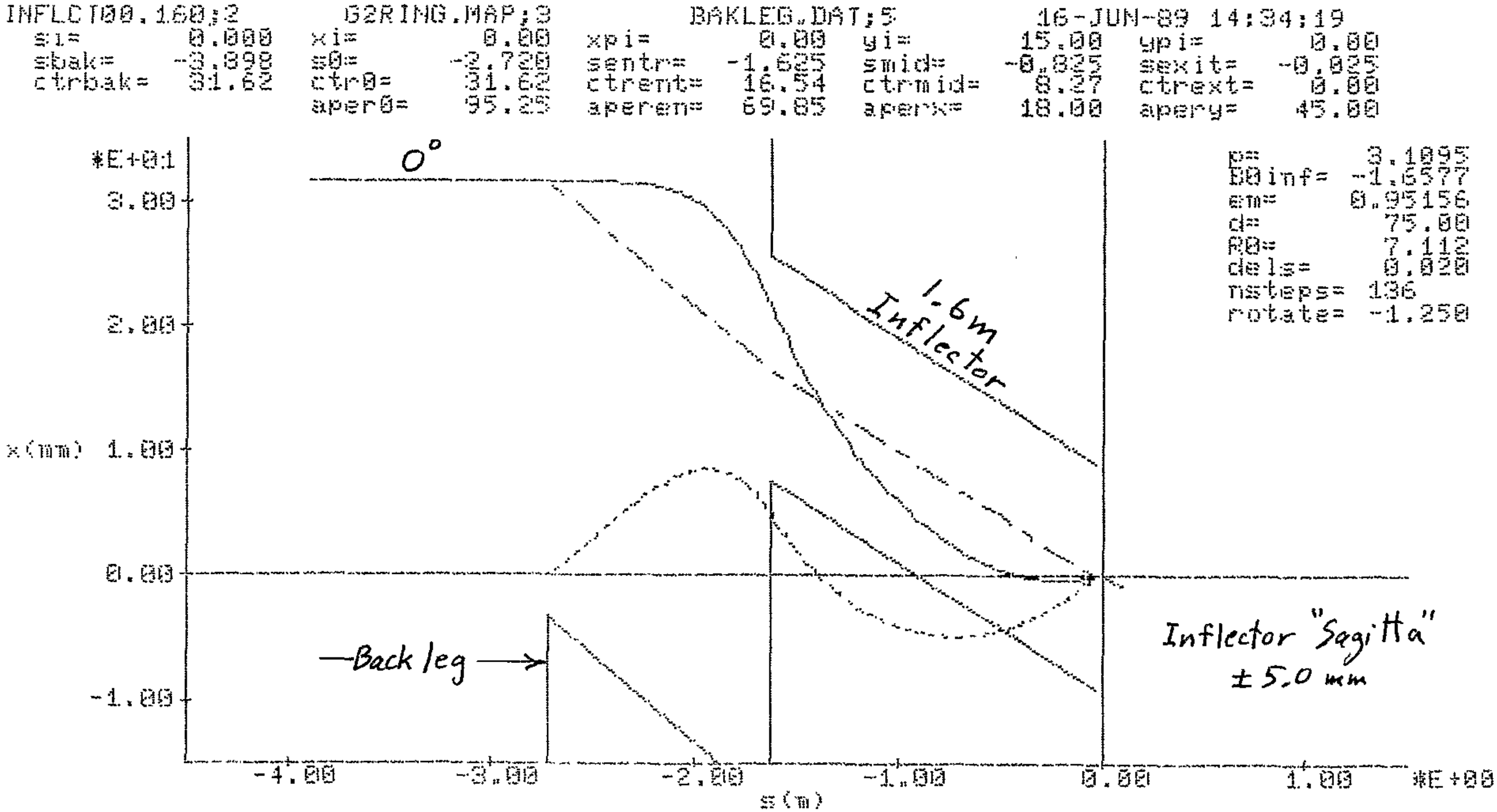

Fig. I.3a Trajectory for 1.7 m Inflector, 0° Approach.

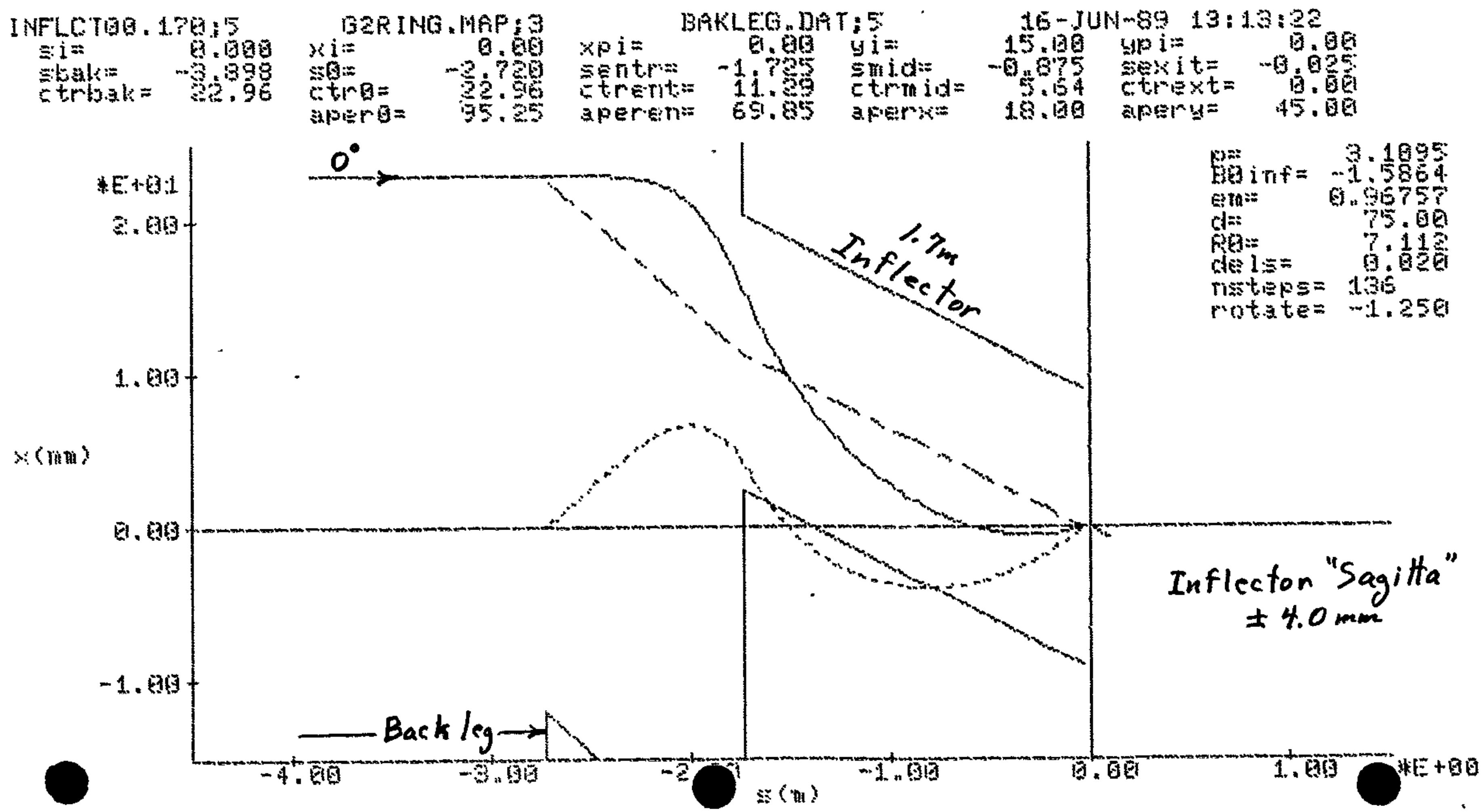

Fig. I.4a Trajectory for 1.8 m Inflector, 0° Approach.

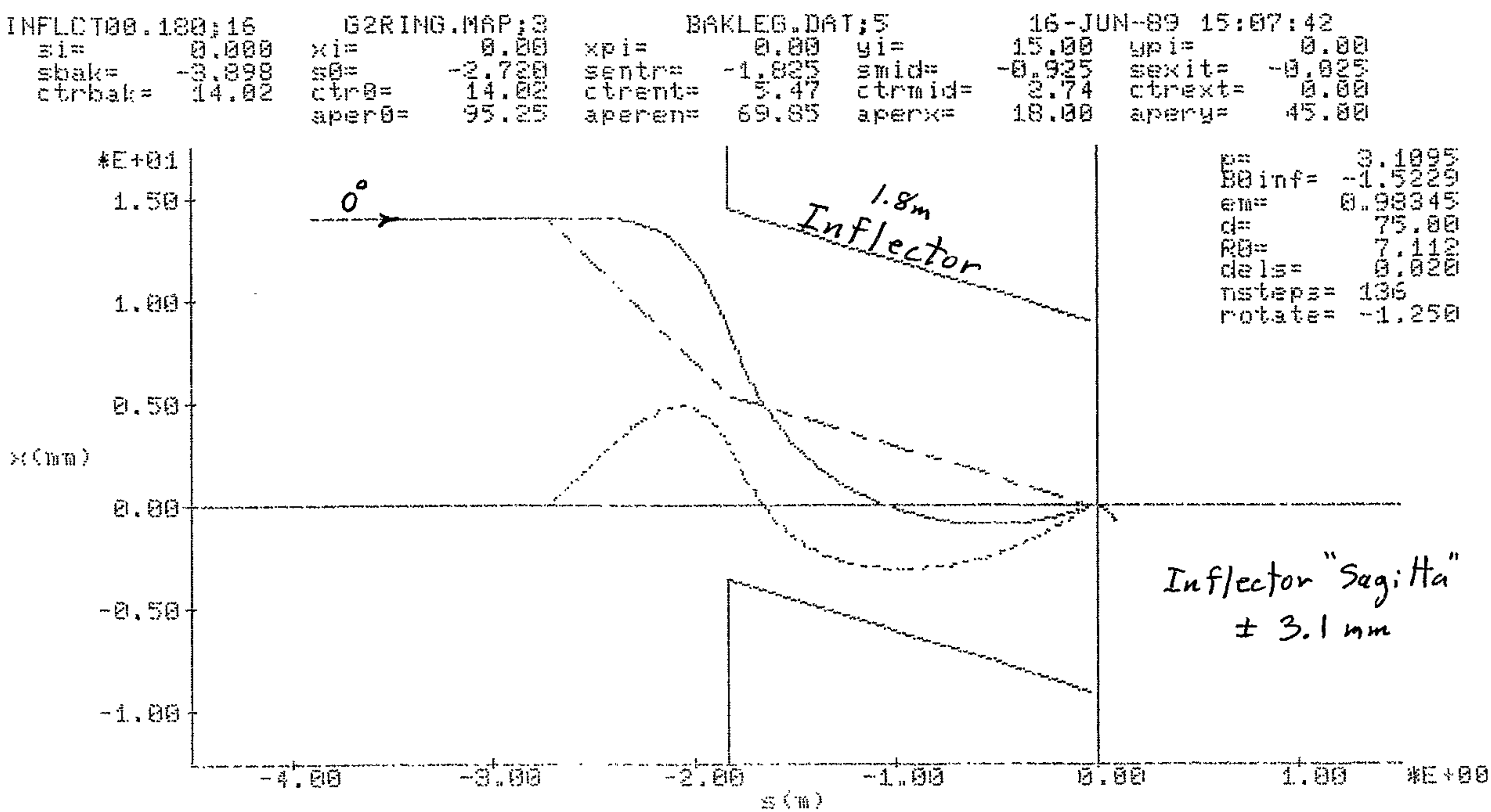

Fig. I.5a Trajectory for 1.6 m Inflector, 1.25° Approach.

```
INFLCT22.160;1        G2RING.MAP;3          BAKLEG.DAT;5           16-JUN-89 14:46:13
  si=      0.000   xi=        0.00   xpi=       0.00   yi=       15.00   ypi=      0.00
  sbak=   -3.898   s0=      -2.720   sentr=   -1.625   smid=    -0.825   sexit=  -0.025
  ctrbak= -26.48   ctr0=     -0.78   ctrent=    7.17   ctrmid=    3.59   ctrext=   0.00
                   aper0=    95.25   aperen=   69.85   aperx=    18.00   apery=   45.00
```

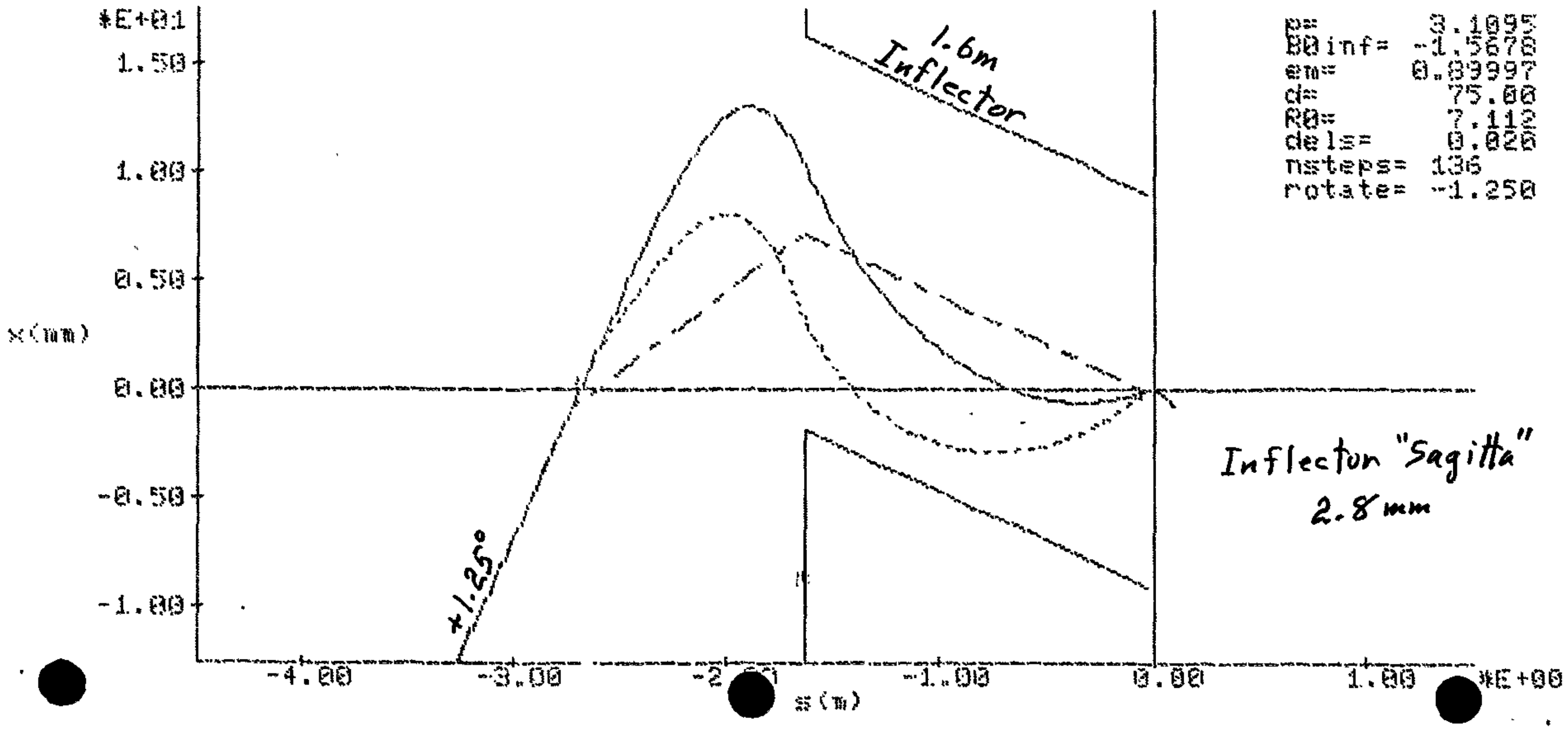

Fig. I.6a Trajectory for 1.7 m Inflector, 1.25° Approach.

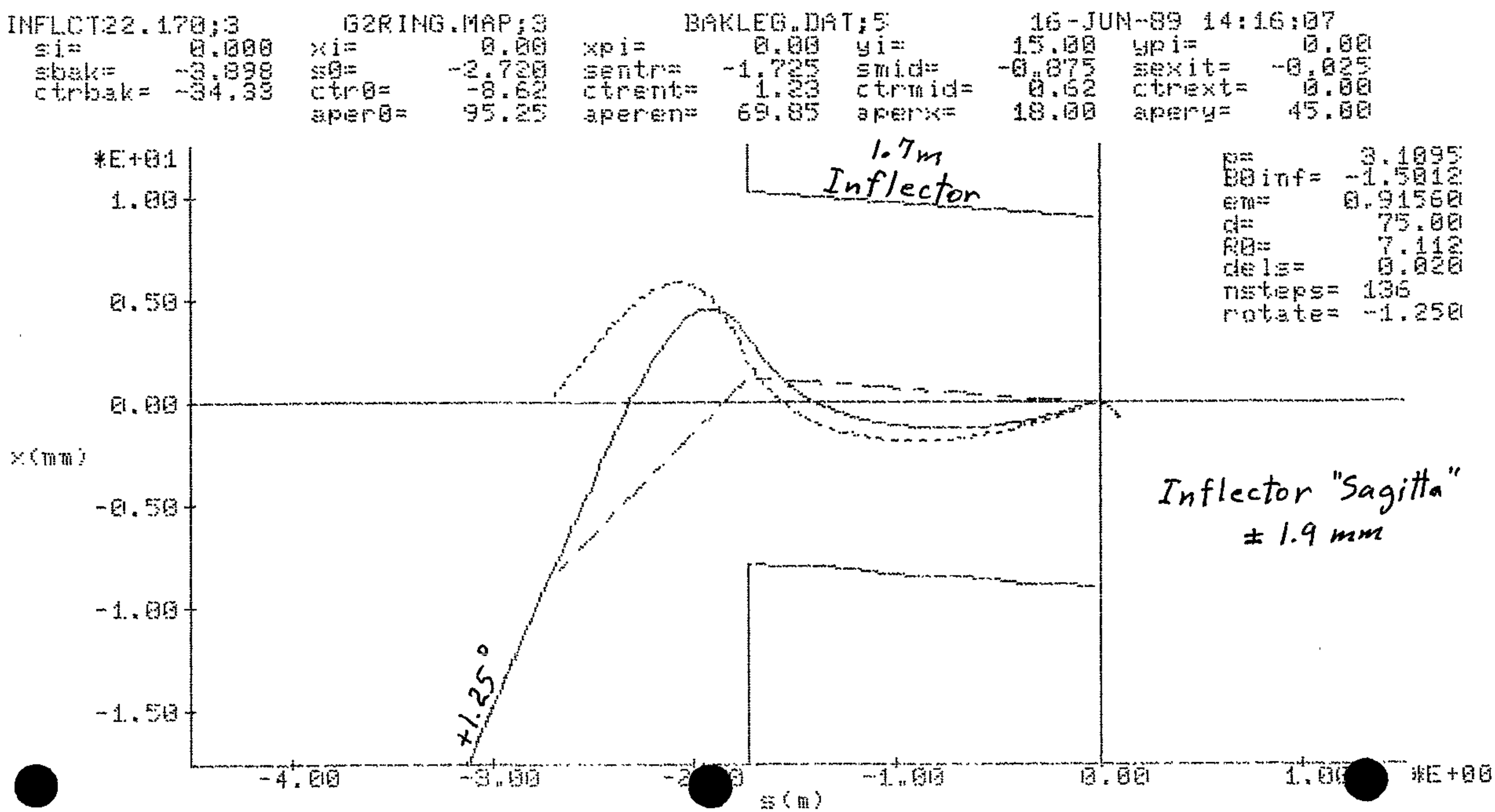

Fig. I.6b Trajectory Between Bolt Holes for 1.7 m Inflector, 1.25° Approach.

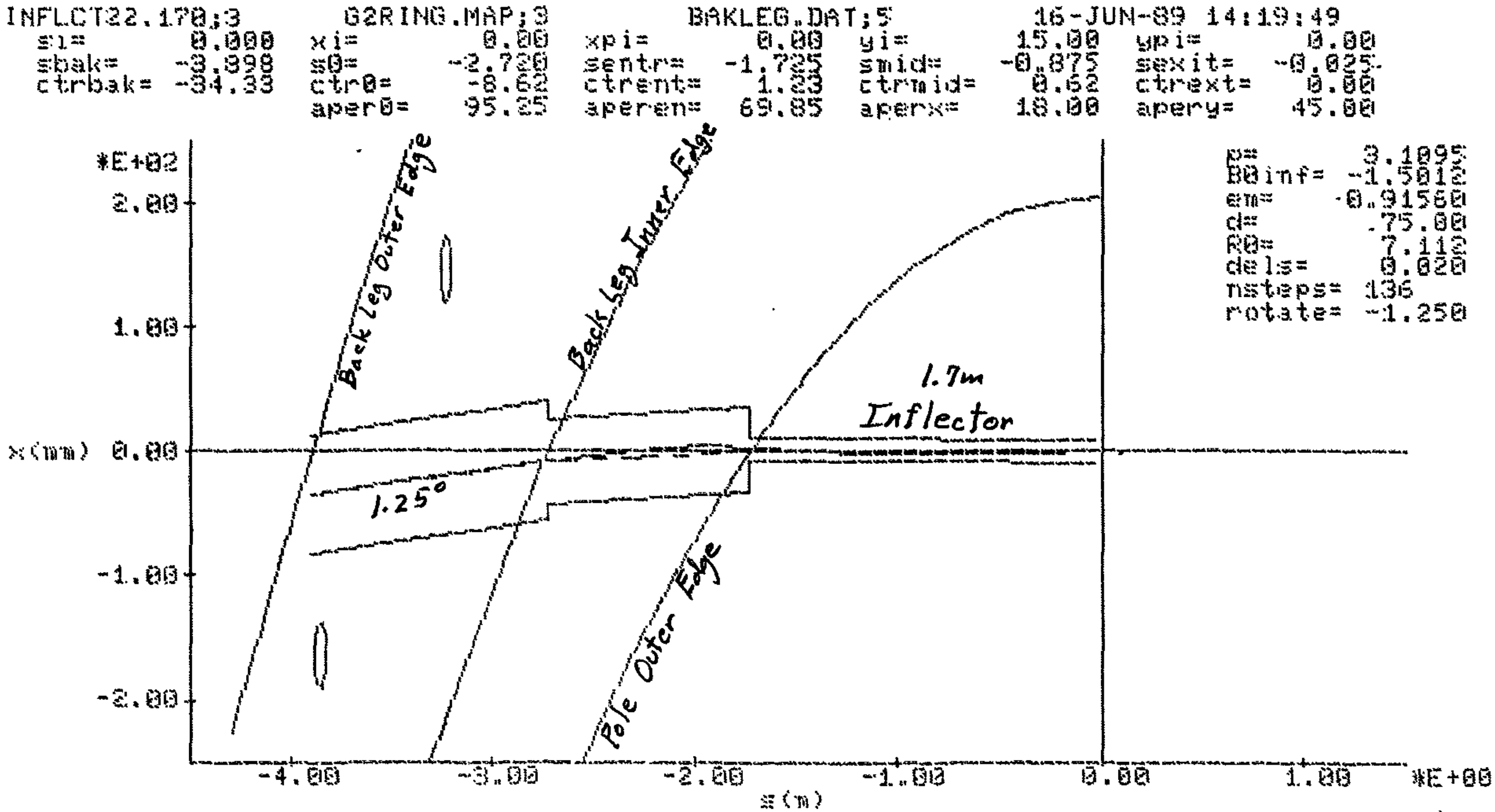

Fig. I.6c Curved Inflector (125 m radius) for Same Trajectory as Fig. I.6a.

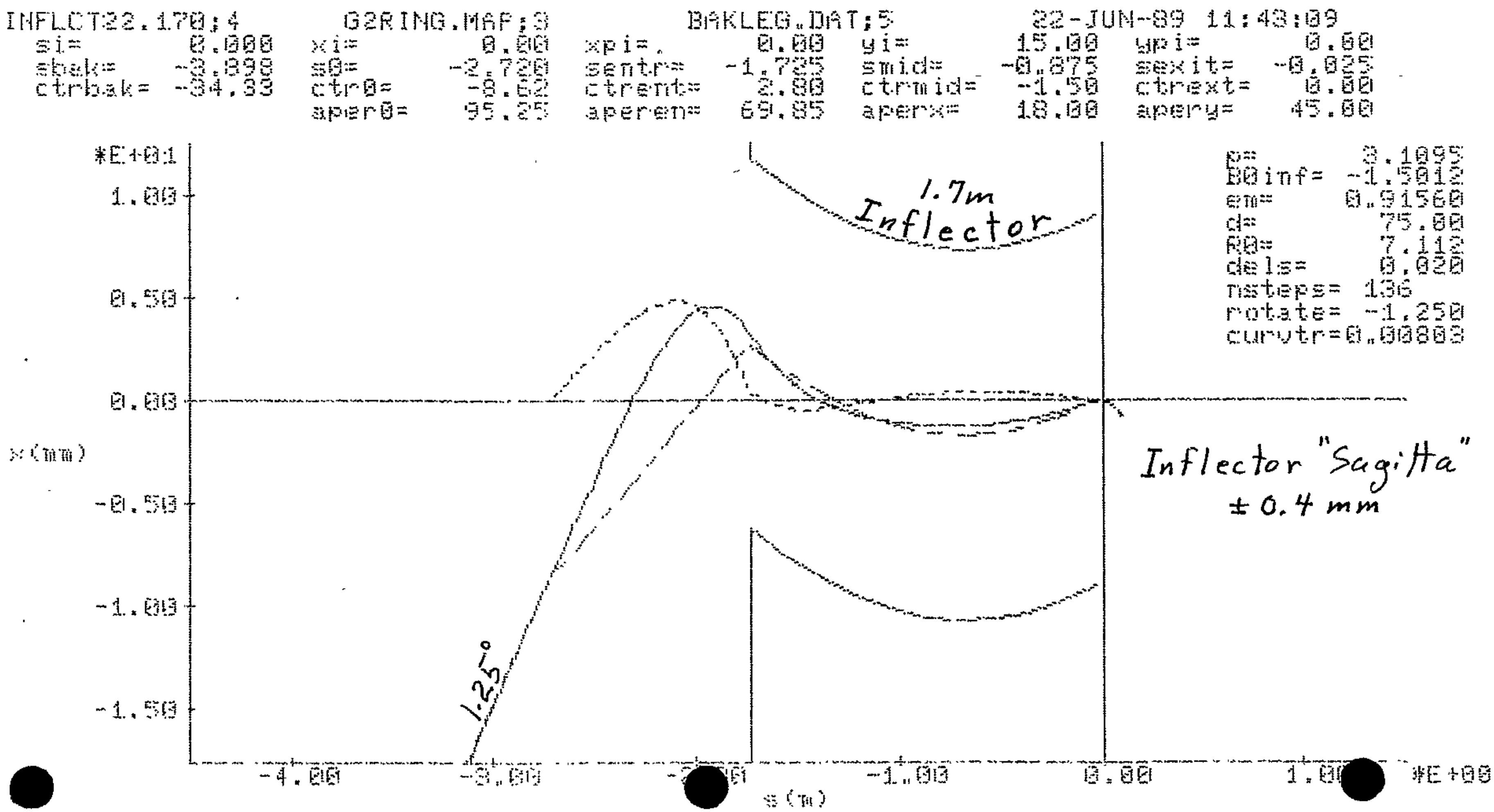

Fig. I.6d Typical Vertical Motion along Trajectory of Fig. I.6a.

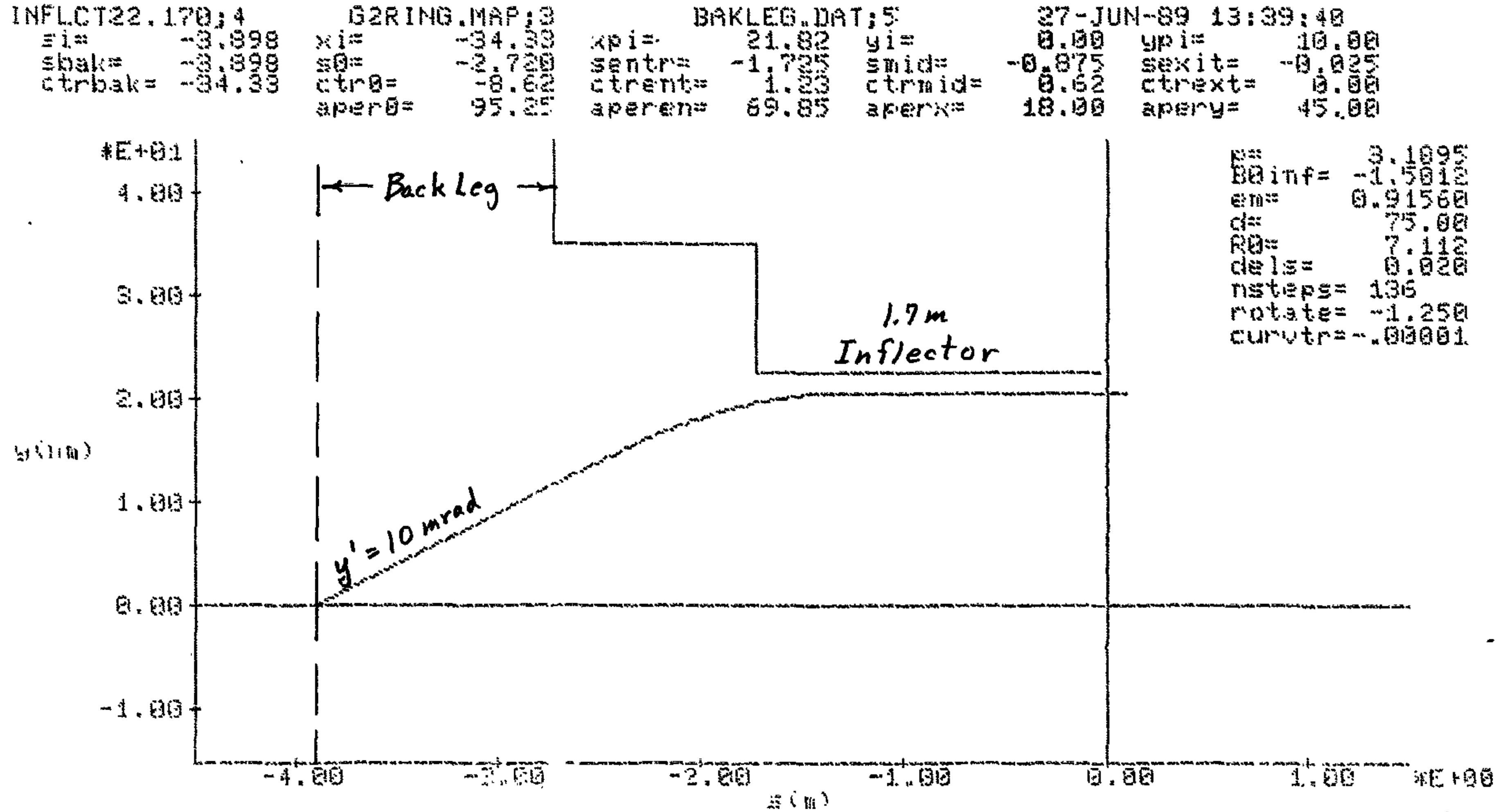

Fig. I.7a Trajectory for 1.8 m Inflector, 1.25° Approach.

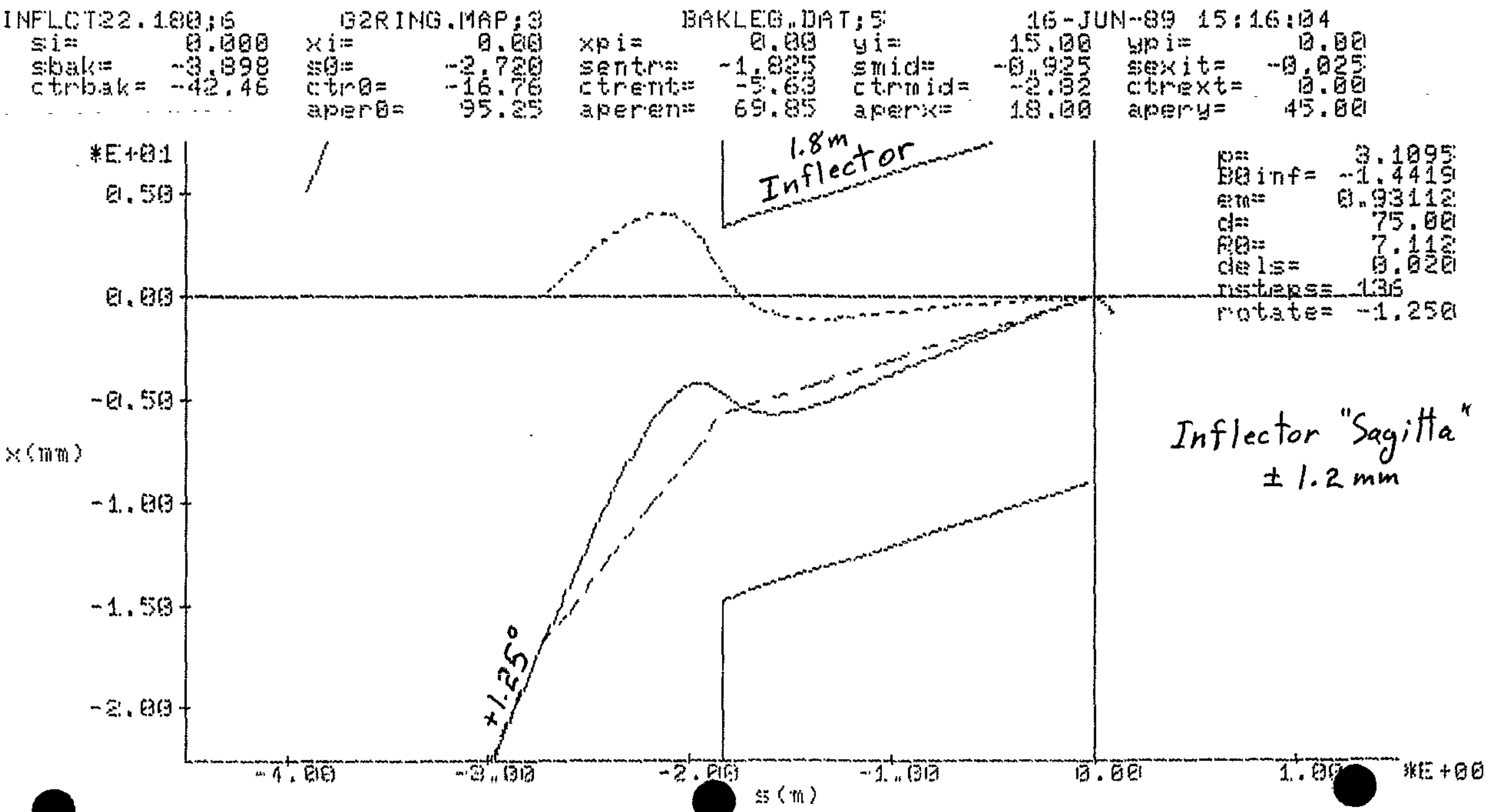

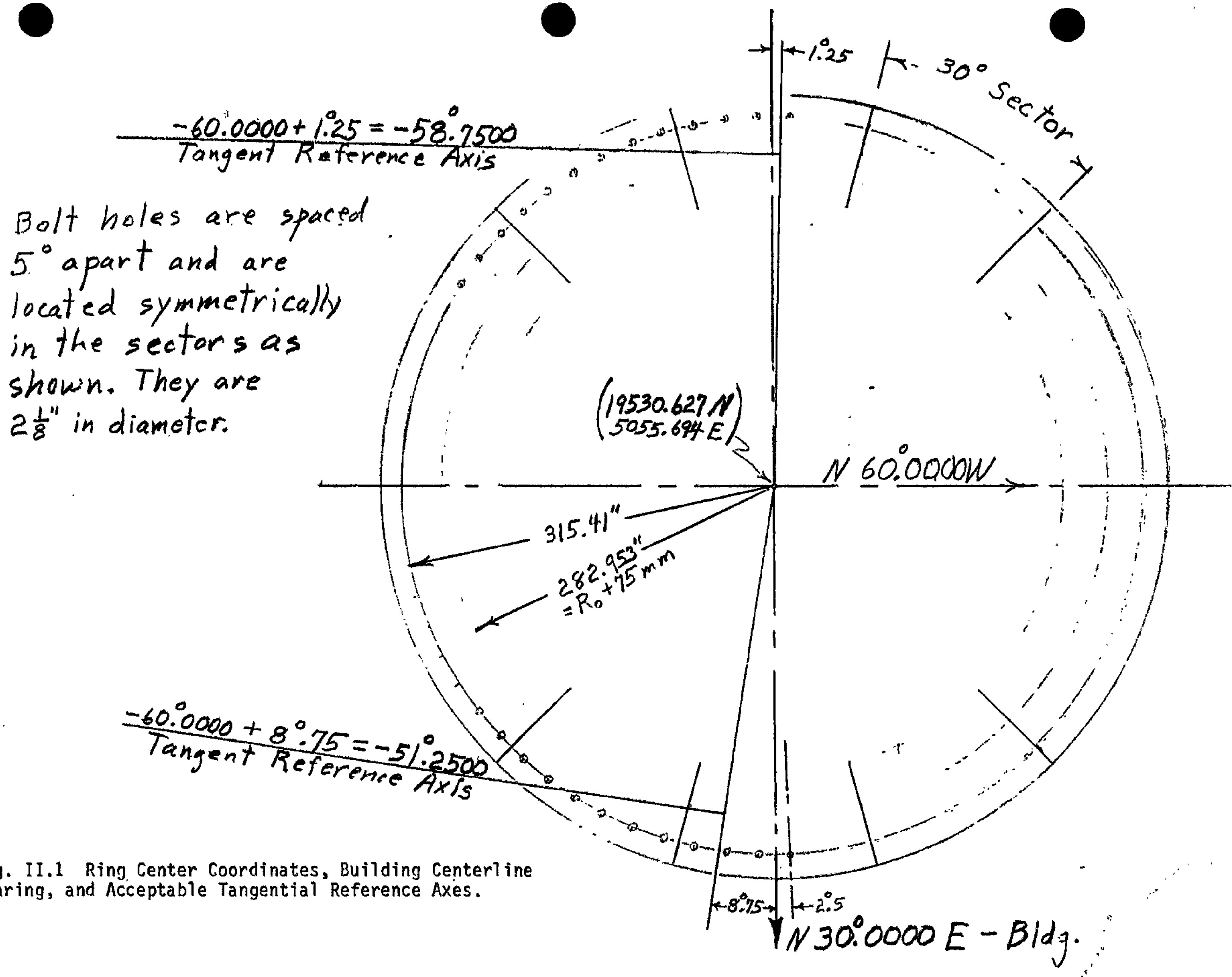

Fig. II.1 Ring Center Coordinates, Building Centerline Bearing, and Acceptable Tangential Reference Axes.

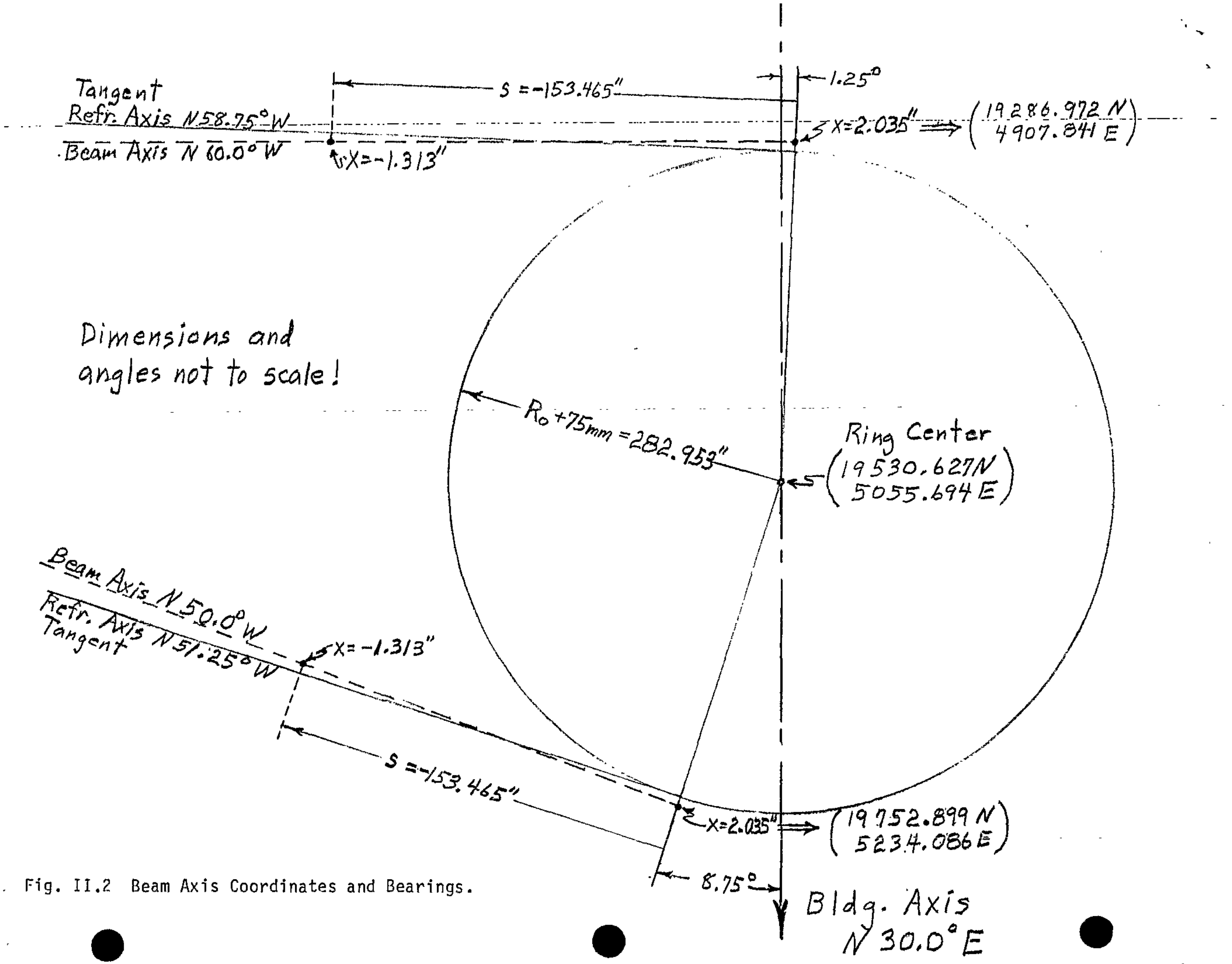

Fig. II.2 Beam Axis Coordinates and Bearings.

Fig. III.1 Variation of Gradient of B_x Along the Tangent Reference Axis.

INFLCT22.170;4		G2RING.MAP;3		BAKLEG.DAT;5		19-JUN-89 14:17:22			
si=	0.000	xi=	0.00	xpi=	0.00	yi=	15.00	ypi=	0.00
sbak=	-3.898	s0=	-2.720	sentr=	-1.725	smid=	-0.875	sexit=	-0.025
ctrbak=	-34.33	ctr0=	-8.62	ctrent=	1.23	ctrmid=	0.62	ctrext=	0.00
		aper0=	95.25	aperen=	69.85	aperx=	18.00	apery=	45.00

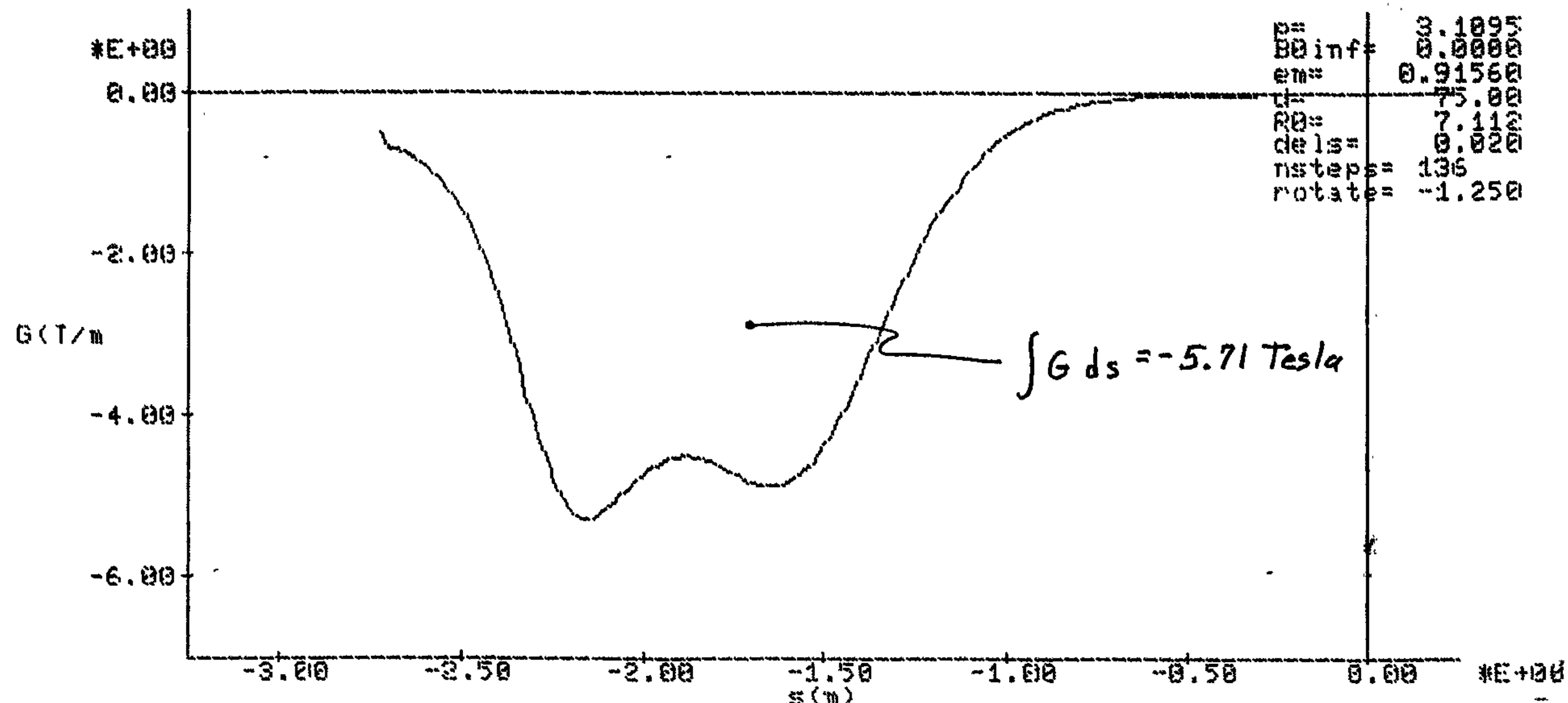

Fig. III.2a Beam Envelopes from Q26 Through Inflector Without Taking Account of Fringe Field Gradient.

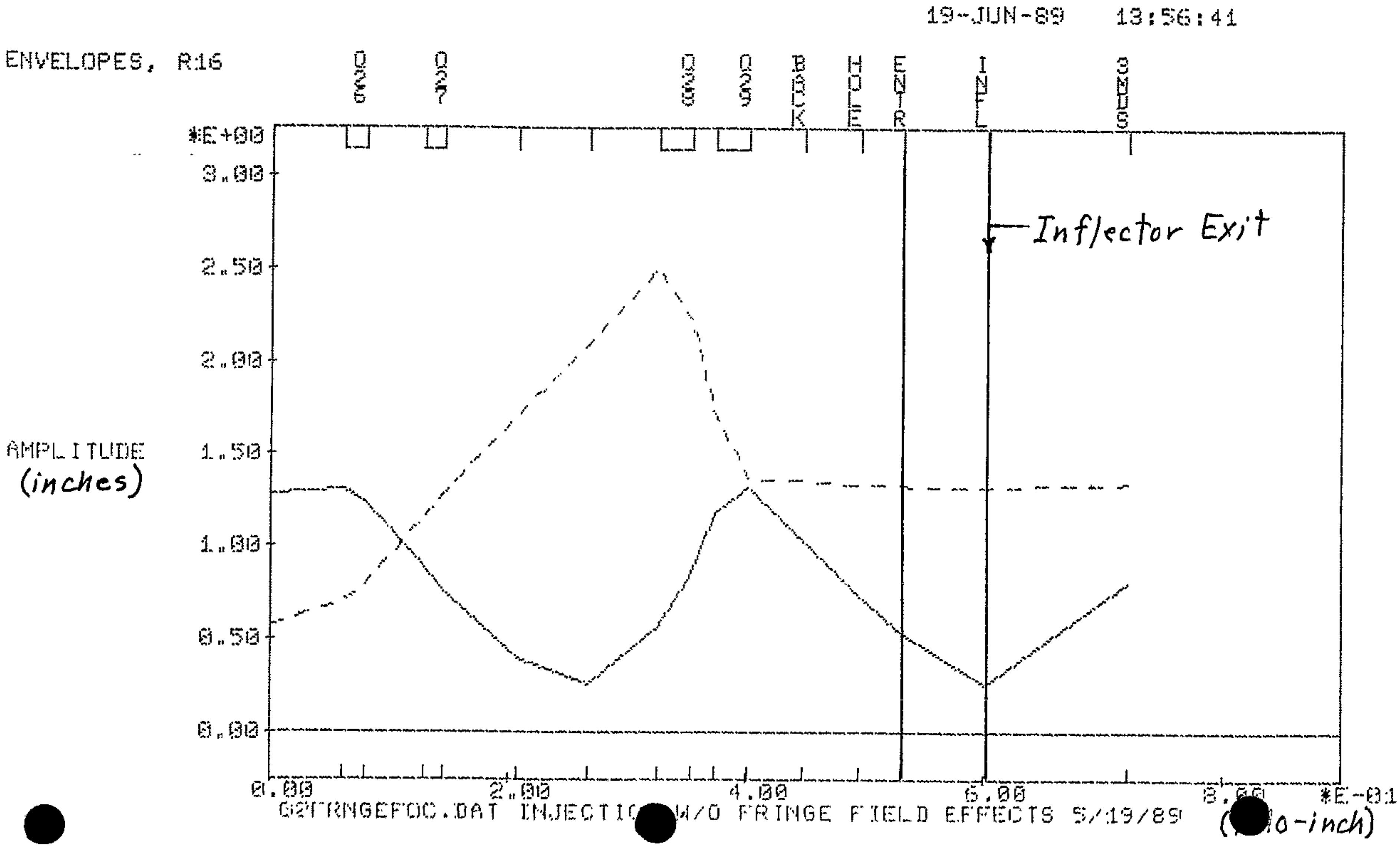

Fig. III.2b Rematched Beam Envelopes [illegible]ing Account of Fringe Field Gradient.

Fringe Field Transforms
From Backleg entry to
Inflector exit:

$$H = \begin{pmatrix} 2.1046 & .23572 \text{ kilo-inch} \\ 15.672 \text{ mrad/in} & 2.2305 \end{pmatrix}$$

$$V = \begin{pmatrix} .0551 & .08054 \\ -12.443 & -.0380 \end{pmatrix}$$

$$(L_2^{-1} H L_1^{-1}) = \begin{pmatrix} .99400 & -.004445 \\ 15.672 & .93603 \end{pmatrix}$$

$$(L_2^{-1} V L_1^{-1}) = \begin{pmatrix} .43692 & .005792 \\ -12.443 & .98981 \end{pmatrix}$$